

High temperature superconductivity in sulfur and selenium hydrides at high pressure

José A. Flores-Livas,¹ Antonio Sanna,¹ and E. K. U. Gross¹

¹*Max-Planck Institut für Mikrostruktur Physics, Weinberg 2, 06120 Halle, Germany*

(Dated: January 29, 2015)

Due to its low atomic mass hydrogen is the most promising element to search for high-temperature phononic superconductors. However, metallic phases of hydrogen are only expected at extreme pressures (400 GPa or higher). The measurement of a record superconducting critical temperature of 190 K in a hydrogen-sulfur compound at 200 GPa of pressure [1], shows that metallization of hydrogen can be reached at significantly lower pressure by inserting it in the matrix of other elements. In this work we re-investigate the phase diagram and the superconducting properties of the H-S system by means of minima hopping method for structure prediction and Density Functional theory for superconductors. We also show that Se-H has a similar phase diagram as its sulfur counterpart as well as high superconducting critical temperature. We predict H₃Se to exceed 120 K superconductivity at 100 GPa. We show that both H₃Se and H₃S, due to the critical temperature and peculiar electronic structure, present rather unusual superconducting properties.

PACS numbers:

Under high pressure conditions, insulating and semi-conducting materials tend to become metallic, because, with increasing electronic density, the kinetic energy grows faster than the potential energy. As metallicity is a necessary condition for superconductivity, superconductivity becomes more likely under pressure [2, 3]. Wigner and Huntington [4], already in 1935 suggested the possibility of a metallic modification of hydrogen under very high pressures. Ashcroft and Richardson predicted [5, 6] hydrogen to become metallic under pressure and also the possibility to be a high temperature superconductor. The high critical temperature (T_C) of hydrogen [7–9] is a consequence of its low atomic mass leading to high energy vibrational modes and in turn to a large phase space available for electron-phonon scattering to induce superconductivity [10]. However, the estimated pressure of metallization [11, 12] is beyond the current experimental capabilities and it has been a challenge to confirm this hypothesis [13–16].

It was only recently that hydrogen-rich compounds started to be explored as a way to decrease the tremendous pressure of metallization in pure hydrogen [17], essentially performing a chemical pre-compression. The first system explored experimentally was silane (SiH₄) [18]. Soon after, many other pre-compressed hydrogen rich materials have been explored experimentally [19–22] and theoretically [23–35]. The importance of a systematic search for a crystalline ground state has been put in evidence for disilane (SiH₆), where structures enthalpically higher lead to transition temperatures of the order of 130 K. Interesting structures have been proved not to be the global minimum and for the correct ground state was found a rather moderate electron-phonon coupling and T_C of 25 K [36]. In agreement with experimental evidence.

Recently it was reported that sulfur hydride (SH₂), when pressurized, becomes metallic and superconduct-

ing. For pressures above 180 GPa an extremely high transition temperature of about 190 K was measured [1]. This T_C is higher than in other superconductors known so far, including cuprates and pnictides. The experimental evidence is supported theoretically [32, 35, 37], and crystal prediction methods suggest that the system becomes superconducting with a SH₃ stoichiometry. In this work we re-investigate extensively the S-H phases with state of the art *ab-initio* material search minima hopping methods [38–40] (MHM) and compute the superconducting properties with the completely parameter-free Density Functional Theory for Superconductors (SCDFT). We also extend the analysis to the Se-H system, predicting a fairly similar phase diagram and comparable superconducting properties.

METHODS

Electronic and phononic structure calculations are performed within density-functional theory as implemented in the two plane-wave based codes ABINIT [41], and ESPRESSO [42] within the local density approximation LDA exchange correlation functional. The core states were accounted for by norm-conserving Troullier-Martins pseudopotentials [43]. The pseudopotential accuracy has been checked against all-electron (LAPW+lo) method as implemented in the ELK code (<http://elk.sourceforge.net/>). In order to predict the ground state structure of sulfur/selenium hydride compounds we use the minima hopping method [38–40] for the prediction of low-enthalpy structures. This method has been successfully used for global geometry optimization in a large variety of applications [44–46]. Given only the chemical composition of a system, the MHM aims at finding the global minimum on the enthalpy surface while gradually exploring low-lying structures. Moves on

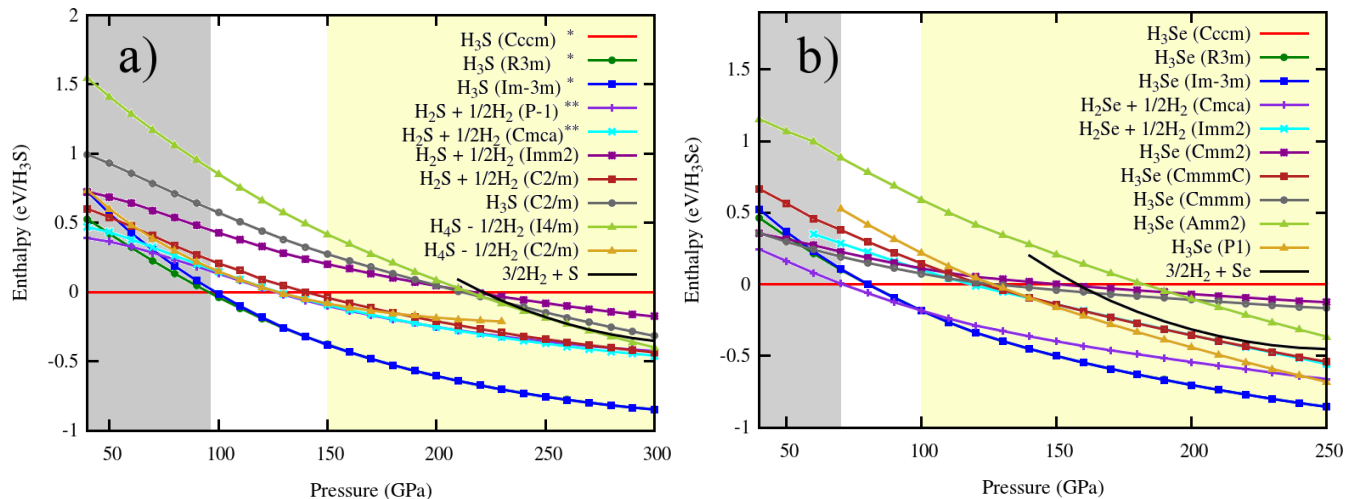


Figure 1. (Color online) Calculated enthalpies for H_3S (a) and H_3Se (b) structures and their decompositions. Values are given with respect to the *Cccm* structure, stable at low pressure. In H_3S three structures were already reported in Ref. 35 (*) and two in Ref. 32 (**). The other structures of H_3S as well as all the structures of H_3Se are predictions of this work by means of the Minima Hopping Method.

the enthalpy surface are performed by using variable cell shape molecular dynamics with initial velocities approximately chosen along soft mode directions. We have used 1,2,3 formula units of H_3S and H_3Se at selected pressures of 100, 150, 200, 250 and 300 GPa. The relaxations to local minima are performed by the fast inertia relaxation engine [47] and both atomic and cell degrees of freedom are taking into account. Final structural relaxations and enthalpy calculations were performed with the VASP code [48]. The plane-wave cutoff energy was set to 800 eV, and Monkhorst-Pack k -point meshes with grid spacing denser than $2\pi \times 0.01 \text{ \AA}^{-1}$, resulting in total energy convergence to better than 1 meV/atom. Superconducting properties have been computed within density-functional theory for superconductors (SCDFT) [49–51]. This theory of superconductivity is completely *ab-initio*, fully parameter-free and proved to be rather accurate and successful in describing phononic superconductors [52–55]. It allows to compute all superconducting properties including the critical temperature and the excitation spectrum of the system [56].

CRYSTAL STRUCTURE PREDICTION AND ENTHALPIES

Experimentally little is known on the high pressure stability and composition of the S-H system and, to the best of our knowledge, nothing is known about the Se-H. Therefore we investigate their low temperature phase diagram by means of the MHM for the prediction of low-enthalpy structures. Computed enthalpies as a function of pressure are reported in Fig. 1. We consider the H_3S stoichiometry as well as its elemental decomposition (sul-

fur + hydrogen), its decomposition into H_2S + hydrogen and H_4S - hydrogen [57]. At low pressure we find the *Cccm* structure up to 95 GPa and the *R3m* (β -Po-type) rhombohedral structure between 95 and 150 GPa. Above 150 GPa, we confirm [32, 37] the cubic *Im* $\bar{3}m$ (bcc) as the most stable lattice.

In a similar way we have studied the Se-H phase diagram. Chemically, selenium is known to have very similar physical properties to sulfur and this system is not an exception. The enthalpies of the phases found in our MHM runs are shown in Fig. 1b. Once again we use the *Cccm* structure as reference since, as in the case of sulfur, it is the most stable at low pressures and up to 70 GPa. Between 70 GPa to 100 GPa, we find that the H_2Se + hydrogen decomposition is more stable than the H_3Se stoichiometry. H_3Se returns to be the most stable composition above 100 GPa and at least up to 250 GPa.

Therefore from our analysis both systems in the range 50 GPa to 250 GPa show, with increasing pressure, two phase transitions. The S-H system, always stable in the H_3S stoichiometry, has a first order phase transition from *Cccm* to *R3m* at ~ 100 GPa, then the *R3m* rhombohedral distortion decreases continuously up to 150 GPa where it transforms into the *Im* $\bar{3}m$ cubic structure. The Se-H system at low pressure is also stable in the H_3Se stoichiometry but becomes unstable to a phase separation into H_2S + hydrogen in the range from 70 GPa to 100 GPa. Above 100 GPa another discontinuous phase transition occurs, directly into the *Im* $\bar{3}m$ cubic structure. Note that 100 GPa is also the pressure below which the *Im* $\bar{3}m$ structure would distort into the β -Po *R3m*, therefore depending on experimental conditions this rhombohedral phase may occur as a metastable one. The sequence

of transformation is highlighted in Fig. 1 by means of shaded areas.

ELECTRONIC AND PHONONIC PROPERTIES OF H_3S AND H_3Se AT HIGH PRESSURE

We focus now on the properties of H_3S and H_3Se in the pressure range of stability of the $Im\bar{3}m$ structure. The two materials present very similar properties. At 200 GPa electronic band dispersions and Fermi surfaces are barely distinguishable, as seen in Fig. 2. And in the range of pressure between 100 to 200 GPa there are no significant changes in the electronic properties apart from the overall bandwidth that increases with pressure. An important aspect of the electronic structure is the presence of several Fermi surface sheets, with no marked nesting features and with Fermi states both at low and high momentum vector. At small momentum (close to the Γ -point, center of the Brillouin zone in Fig. 2) there are three small Fermi surfaces (only the green larger one can be seen in the figure, smaller ones being inside it). However, these provide a rather small contribution to the total density of states (DOS) at the Fermi level which mostly comes from the two larger Fermi surface sheets. These are of *hybrid* character, meaning that their Kohn-Sham (KS) states overlap both with H and S/Se states (the overlap is expressed in the figure by the color-scale of the band lines), suggesting that they will be coupled with both hydrogen and S/Se lattice vibrations (more details on this point will be given in the next section). Overall the DOS shows a square root behavior of the 3D electron gas, the main deviation from this occurs close to the Fermi energy where a peak with an energy width of about 2 eV is present. This structure will play a relevant role in the superconducting properties.

Unlike the electronic structure, phonons are strongly pressure and material dependent. Clearly a key role is played by the occurrence of the II order $R\bar{3}m$ to $Im\bar{3}m$ phase transition. Far away from it (i.e. at very high pressure) we have three sets of well separated phonon modes: acoustic (below 60 meV), optical modes that are transverse with respect to the S/Se-H bond (between 100 to 200 meV) and, above 200 meV, stretching modes of the Se/S-H bond. These are clearly seen in Fig. 3b for H_3Se at 200 GPa. As pressure reduces, the bond structure of the system tends to destabilize because, from a four-fold coordination in the $Im\bar{3}m$ structure, it goes to a three-fold coordination in the $R\bar{3}m$ one. This means that one of the high-energy stretching mode slowly softens at Γ . This softening can be clearly seen in H_3S at 200 GPa (Fig. 3a) where a H-S stretching mode went down to about 60 meV. Eventually, as pressure lowers this softens to zero energy, marking the occurrence of the phase transition, at about 150 GPa in H_3S and slightly below 100 GPa in H_3Se . In fact, at 100 GPa this mode has, in H_3Se , almost zero

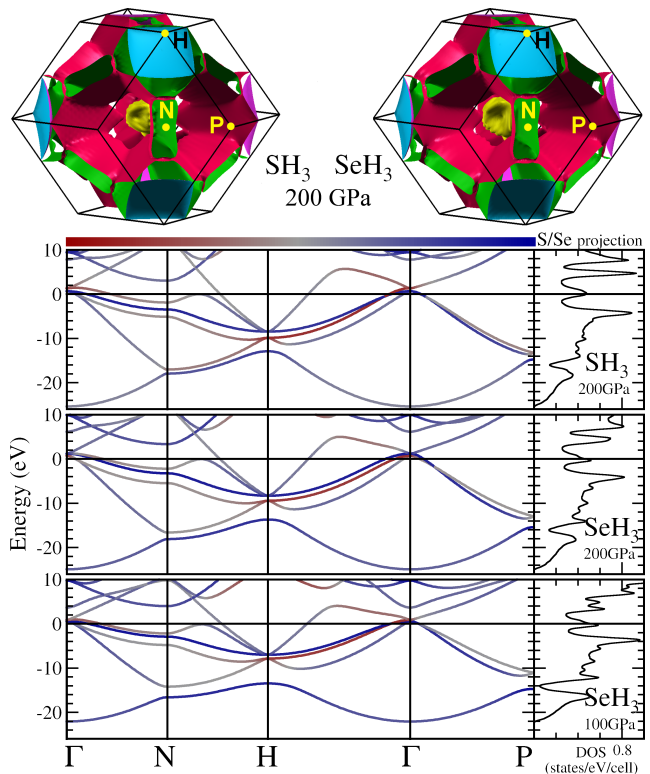


Figure 2. (Color online) Fermi Surfaces (top) and electronic band structures (bottom) of H_3S and H_3Se at high pressure in the $Im\bar{3}m$ phase. The color-scale in the band lines indicates the projection of the KS states on the atomic orbitals of the sulfur/selenium atom normalized by the maximum total atomic projection of these valence states that is of about 70%.

energy (see Fig. 3c).

In spite of these important changes in the phononic energy dispersion, the overall coupling strength^[58, 59] λ does not show large variations over the pressure range, as we can see from Tab. I. Naturally the coupling increases near the phase transition due the optical mode softening, however, as this is restricted to a relatively small region near the Γ point, the effect is not dramatic. On the other hand there is definitively a difference in the coupling strength of the Se ($\lambda \sim 1.5$) with respect to the S system ($\lambda \sim 2.5$), indicating that selenium, due to its larger ionic size, provides a better electronic screening of the hydrogen vibrations.

SUPERCONDUCTING PROPERTIES

We have computed, by means of SCDFE, critical temperatures of H_3S and H_3Se in the pressure range of stability of the $Im\bar{3}m$ structure, these are collected in Tab. I. The predicted T_C for the H_3S system is 180 K at 200 GPa and 195 K at 180 GPa, in agreement with the measured value of 185 K at 177 GPa. On the other hand our predic-

tion for the deuterium substituted system D_3S is 141 K, at 200 GPa. That is much larger than the measured [1] T_C of 90 K. This huge experimental isotope effect is therefore not consistent with our calculations. However the good agreement obtained with the T_C of the H_3S system seem to exclude an explanation in terms of anharmonic effects in the hydrogen vibrations, as suggested in Ref. 60. Nevertheless, the theoretical isotope coefficients $\alpha^S = 0.05$ and $\alpha^H = 0.4$ (defined as $\alpha^A = -\frac{M^A}{T_C} \frac{\partial T_C}{\partial M^A}$, and computed at 200 GPa with a three point numerical differentiation) clearly indicate and confirm [60] the dominant contribution of hydrogen phonon modes to the superconducting pairing.

Our prediction for H_3Se at 200 GPa is of 131 K, this reduction of T_C is clearly not an isotopic effect of the substitution S to Se. As mentioned in the previous section, it is caused, instead, by a different coupling strength of the hydrogen modes in the Se environment. In spite of the much lower coupling strength λ the reduction of T_C is not very large with respect to the sulfur system, as expected from the fact that the critical temperature at high coupling increases with the square root of λ (while is exponential at low coupling) [58, 59].

To compute the critical temperatures we have used SCDFt, this choice allow us to deal with the unusual superconducting properties of these systems from first principles without relying on conventional assumptions coming from low pressure experience. There are two aspects of these systems that are uncommon, that make the use of conventional [61] Eliashberg methods difficult to apply to these systems. First, the strong variation of the electronic density of states at the Fermi level, that is pinned to a rather sharp peak in the DOS, second the extremely large el-ph coupling and phonon frequencies that lead to a very broad region around E_F where the interaction is dominated by phonons over Coulomb repulsion.

The effect of the energy dependence of the DOS can be appreciated by comparing Eliashberg results with SCDFt when neglecting the Coulomb interaction (see Tab. I). At 200 GPa the two theories [65] disagree by 54 K, SCDFt giving 284 K while Eliashberg gives 338 K. This difference comes from the energy dependence of the DOS, while Eliashberg assumes a flat DOS, in the SCDFt we can easily check this assumption by assuming a flat DOS, and for this case the SCDFt calculation would lead to 334 K, in agreement with the Eliashberg result.

Physically the reduction of T_C , occurring when the real DOS is considered, arises from the fact that the phononic pairing extends in a rather large region around the Fermi level, over the DOS peak structure of these systems (see Fig. 2). Beyond the range of the phononic pairing the coupling is dominated by the Coulomb interaction. As, in the static limit, this is repulsive, a superconducting system compensates it by a phase shift in the gap (i.e. in the quasiparticle orbitals), therefore making this repul-

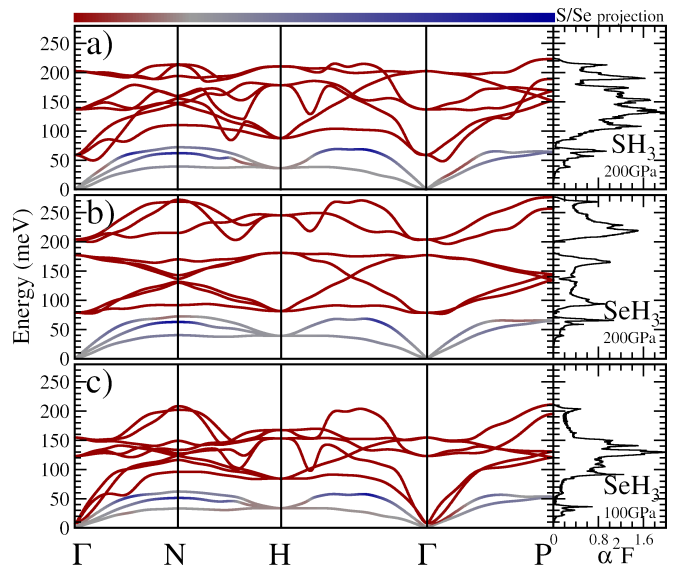


Figure 3. (Color online) Phonon dispersion and α^2F functions [58, 59] of H_3S and H_3Se at high pressure in the cubic $Im\bar{3}m$ structure. The color coding gives the projection of the mode displacement on the S/Se atom. Displacements are visible dominated by H due to its lighter mass.

sion contribute to the condensation (in unconventional superconductors exactly the same happens but directly at the Fermi level). This mechanism is called Coulomb renormalization [59] since it *renormalizes* the repulsive Coulomb scattering that occurs at low energy. The phase shift occurs at $|\epsilon_{\mathbf{k}}| \gtrsim \omega_{log}$ but the scattering processes become less and less important as $|\epsilon_{\mathbf{k}}|$ increases (going down as $1/\epsilon$). Therefore the most important energy region is where the DOS of the H_3S and H_3Se systems shows a dip, implying that the phase space available for this process is small and its effect weak. Note that in order to reproduce the T_C coming from SCDFt within the Allen-Dynes (AD) formula one should assume a μ^* of 0.16, that is actually much larger than the value of μ itself ($\simeq 0.1$). Making clear that the the Morel-Anderson theory [66] can not even be applied.

The superconducting pairing is distributed over many phonon modes and over the Brillouin zone in \mathbf{q} -space, despite the presence of several Fermi surface sheets and with different orbital character across the Fermi level, we obtained a isotropic (weakly \mathbf{k} -dependent) gap at the Fermi level and the effect of anisotropy [67] on T_C is negligible (< 1 K).

CONCLUSIONS

We have presented a theoretical investigation on the crystal structure and superconductivity of H_3S . An extensive structural search confirms the H_3S stoichiometry as the most stable configuration at high pressure. By

		λ	ω_{log}	T_c^{SCDFT}	$\Delta(T=0)$	$T_c^{SCDFT,ph}$	$T_c^{AD,\mu^*=0.1}$	$T_c^{AD,\mu^*=0}$
H ₃ S	200 GPa	2.41	109 meV	180 K	43.8 meV	284 K	255 K	338 K
D ₃ S	200 GPa	2.41	82 meV	141 K	32.9 meV	216 K	188 K	247 K
H ₃ S	180 GPa	2.57	101 meV	195 K	44.8 meV	297 K	250 K	331 K
H ₃ Se	200 GPa	1.45	120 meV	131 K	28.4 meV	234 K	174 K	246 K
H ₃ Se	150 GPa	1.38	107 meV	110 K	23.4 meV	195 K	145 K	209 K
H ₃ Se	100 GPa	1.76	87 meV	123 K	27.0 meV	198 K	156 K	214 K

Table I. Calculated critical Temperatures and gaps. λ is the electron phonon coupling parameter [58, 59]; ω_{log} is the logarithmic average of the α^2F function [58, 59]; T_c^{SCDFT} is the critical temperature from SCDFT including RPA screened Coulomb repulsion; $T_c^{SCDFT,ph}$ is the phonon only SCDFT critical temperature; $T_c^{AD,\mu^*=0}$ is the critical temperature from the Allen-Dynes modified McMillan formula [59, 62, 63], at $\mu^* = 0$ (i.e. with no Coulomb pairing); $T_c^{AD,\mu^*=0.1}$ is the same AD formula but with the conventional value of $\mu^* = 0.1$; $\Delta(T=0)$ is the superconducting gap computed [64] from the SCDFT calculations

means of parameter-free SCDFT we have predicted a T_C of 180 K at 200 GPa, in excellent agreement with experimental results. This confirms H₃S to be the material with the highest known superconducting critical temperature. The mechanism of superconductivity is clearly the same that was predicted for metallic hydrogen[5, 7, 9]: the combine effect of high characteristic frequency due to hydrogen light mass and strong coupling due to the lack of electronic core in hydrogen. Still the working pressures of this superconductor is too high for any technological application [68]. Nevertheless the discovery of metallic superconducting hydrogenic bands already at 150 GPa gives hope that further theoretical and experimental research in this direction may lead to even lower hydrogen metallization pressures and higher temperature superconductivity. Here we predict that H₃S is stable in the cubic *Im3m* already at 100 GPa with a very high T_C of 123 K, a value which is comparable to the cuprate superconductors.

J.A.F.L. acknowledge fruitful discussion with Maximilian Amsler on crystal prediction and the financial support from EU's 7th framework Marie-Sklodowska-Curie scholarship program within the "ExMaMa" Project (329386)

[1] A. Drozdov, M. I. Erements, and I. A. Troyan, [arXiv:1412.0460 \[cond-mat.supr-con\]](https://arxiv.org/abs/1412.0460) (2014).
[2] K. Shimizu, K. Amaya, and N. Suzuki, *Journal of the Physical Society of Japan* **74**, 1345 (2005), <http://dx.doi.org/10.1143/JPSJ.74.1345>.
[3] C. Buzea and K. Robbie, *Superconductor Science and Technology* **18**, R1 (2005).
[4] E. Wigner and H. B. Huntington, *The Journal of Chemical Physics* **3**, 764 (1935).
[5] N. Ashcroft, *Phys. Rev. Lett.* **21**, 1748 (1968).
[6] C. F. Richardson and N. W. Ashcroft, *Phys. Rev. Lett.* **78**, 118 (1997).
[7] P. Cudazzo, G. Profeta, A. Sanna, A. Floris, A. Continenza, S. Massidda, and E. Gross, *Phys. Rev. Lett.* **100**, 257001 (2008).

[8] L. Zhang, Y. Niu, Q. Li, T. Cui, Y. Wang, Y. Ma, Z. He, and G. Zou, *Solid State Communications* **141**, 610 (2007).
[9] P. Cudazzo, G. Profeta, A. Sanna, A. Floris, A. Continenza, S. Massidda, and E. K. U. Gross, *Phys. Rev. B* **81**, 134505 (2010).
[10] J. Bardeen, L. N. Cooper, and J. R. Schrieffer, *Phys. Rev.* **108**, 1175 (1957).
[11] C. J. Pickard and R. J. Needs, *Nat Phys* **3**, 473 (2007).
[12] P. Cudazzo, G. Profeta, A. Sanna, A. Floris, A. Continenza, S. Massidda, and E. Gross, *Phys. Rev. B* **81**, 134506 (2010).
[13] P. Loubeyre, F. Occelli, and R. LeToullec, *Nature* **416**, 13 (2002).
[14] M. I. Erements and I. A. Troyan, *Nat. Mat.* **10**, 927 (2011).
[15] C.-S. Zha, Z. Liu, and R. Hemley, *Phys. Rev. Lett.* **108**, 146402 (2012).
[16] I. I. Naumov and R. J. Hemley, *Accounts of Chemical Research* **47**, 3551 (2014), pMID: 25369180, <http://dx.doi.org/10.1021/ar5002654>.
[17] N. Ashcroft, *Phys. Rev. Lett.* **92**, 187002 (2004).
[18] M. I. Erements, I. A. Trojan, S. A. Medvedev, J. S. Tse, and Y. Yao, *Science* **319**, 1506 (2008).
[19] X. Chen, V. V. Struzhkin, Y. Song, A. F. Goncharov, M. Ahart, Z. Liu, H.-k. Mao, and R. J. Hemley, *Proceedings of the National Academy of Sciences* **105**, 20 (2008).
[20] O. Degtyareva, J. E. Proctor, C. L. Guillaume, E. Gregoryanz, and M. Hanfland, *Solid State Communications* **149**, 1583 (2009).
[21] M. Hanfland, J. E. Proctor, C. L. Guillaume, O. Degtyareva, and E. Gregoryanz, *Phys. Rev. Lett.* **106**, 095503 (2011).
[22] T. Strobel, P. Ganesh, M. Somayazulu, P. Kent, and R. Hemley, *Phys. Rev. Lett.* **107**, 255503 (2011).
[23] J. S. Tse, Y. Yao, and K. Tanaka, *Phys. Rev. Lett.* **98**, 117004 (2007).
[24] X.-J. Chen, V. V. Struzhkin, Y. Song, A. F. Goncharov, M. Ahart, Z. Liu, H.-k. Mao, and R. J. Hemley, *Proceedings of the National Academy of Sciences* **105**, 20 (2008).
[25] D. Y. Kim, R. H. Scheicher, S. LeB̄ague, J. Prasongkit, B. Arnaud, M. Alouani, and R. Ahuja, *Proceedings of the National Academy of Sciences* **105**, 16454 (2008).
[26] S. Wang, H.-k. Mao, X.-J. Chen, and W. L. Mao, *Proceedings of the National Academy of Sciences* **106**, 14763 (2009).

- [27] Y. Yao and D. D. Klug, *Proceedings of the National Academy of Sciences* **107**, 20893 (2010).
- [28] G. Gao, A. R. Oganov, P. Li, Z. Li, H. Wang, T. Cui, Y. Ma, A. Bergara, A. O. Lyakhov, T. Iitaka, and G. Zou, *Proceedings of the National Academy of Sciences* **107**, 1317 (2010).
- [29] D. Y. Kim, R. H. Scheicher, H.-k. Mao, T. W. Kang, and R. Ahuja, *Proceedings of the National Academy of Sciences* **107**, 2793 (2010).
- [30] Y. Li, G. Gao, Y. Xie, Y. Ma, T. Cui, and G. Zou, *Proceedings of the National Academy of Sciences* **107**, 15708 (2010).
- [31] D. Zhou, X. Jin, X. Meng, G. Bao, Y. Ma, B. Liu, and T. Cui, *Phys. Rev. B* **86**, 014118 (2012).
- [32] Y. Li, J. Hao, H. Liu, Y. Li, and Y. Ma, *The Journal of Chemical Physics* **140**, (2014).
- [33] Y. Wang and Y. Ma, *The Journal of Chemical Physics* **140**, 040901 (2014).
- [34] J. Hooper, T. Terpstra, A. Shamp, and E. Zurek, *The Journal of Physical Chemistry C* **118**, 6433 (2014).
- [35] D. Duan, Y. Liu, F. Tian, D. Li, X. Huang, Z. Zhao, H. Yu, B. Liu, W. Tian, and T. Cui, *Sci. Rep.* **4** (2005), <http://dx.doi.org/10.1038/srep06968>.
- [36] M. Amsler, J. A. Flores-Livas, L. Lehtovaara, F. Balima, S. A. Ghasemi, D. Machon, S. Pailhès, A. Willand, D. Caliste, S. Botti, A. San Miguel, S. Goedecker, and M. A. L. Marques, *Phys. Rev. Lett.* **108**, 065501 (2012).
- [37] N. Bernstein, C. S. Hellberg, M. D. Johannes, I. I. Mazin, and M. J. Mehl, ArXiv e-prints (2015), [arXiv:1501.00196](https://arxiv.org/abs/1501.00196) [cond-mat.supr-con].
- [38] S. Goedecker, *The Journal of Chemical Physics* **120**, 9911 (2004).
- [39] S. Goedecker, W. Hellmann, and T. Lenosky, *Phys. Rev. Lett.* **95**, 055501 (2005).
- [40] M. Amsler and S. Goedecker, *The Journal of Chemical Physics* **133**, 224104 (2010).
- [41] X. Gonze, B. Amadon, P. Anglade, J. Beuken, F. Bottin, P. Boulanger, F. Bruneval, D. Caliste, R. Caracas, M. Côté, T. Deutsch, L. Genovese, P. Ghosez, M. Giantomassi, S. Goedecker, D. Hamann, P. Hermet, F. Jollet, G. Jomard, S. Leroux, M. Mancini, S. Mazevet, M. Oliveira, G. Onida, Y. Pouillon, T. Rangel, G. Rigamane, D. Sangalli, R. Shaltaf, M. Torrent, M. Verstraete, G. Zerah, and J. Zwanziger, *Computer Physics Communications* **180**, 2582 (2009).
- [42] P. Giannozzi, S. Baroni, N. Bonini, M. Calandra, R. Car, C. Cavazzoni, D. Ceresoli, G. L. Chiarotti, M. Cococcioni, I. Dabo, A. Dal Corso, S. de Gironcoli, S. Fabris, G. Fratesi, R. Gebauer, U. Gerstmann, C. Gougoussis, A. Kokalj, M. Lazzeri, L. Martin-Samos, N. Marzari, F. Mauri, R. Mazzarello, S. Paolini, A. Pasquarello, L. Paulatto, C. Sbraccia, S. Scandolo, G. Sclauzero, A. P. Seitsonen, A. Smogunov, P. Umari, and R. M. Wentzcovitch, *Journal of Physics: Condensed Matter* **21**, 395502 (19pp) (2009).
- [43] M. Fuchs and M. Scheffler, *Comput. Phys. Commun.* **119**, 67 (1999).
- [44] M. Amsler, J. A. Flores-Livas, L. Lehtovaara, F. Balima, S. A. Ghasemi, D. Machon, S. Pailhès, A. Willand, D. Caliste, S. Botti, A. San Miguel, S. Goedecker, and M. A. L. Marques, *Phys. Rev. Lett.* **108**, 065501 (2012).
- [45] M. Amsler, J. A. Flores-Livas, T. D. Huan, S. Botti, M. A. L. Marques, and S. Goedecker, *Phys. Rev. Lett.* **108**, 205505 (2012).
- [46] S. Botti, J. A. Flores-Livas, M. Amsler, S. Goedecker, and M. A. L. Marques, *Phys. Rev. B* **86**, 121204 (2012).
- [47] E. Bitzek, P. Koskinen, F. Gähler, M. Moseler, and P. Gumbsch, *Phys. Rev. Lett.* **97**, 170201 (2006).
- [48] G. Kresse and J. Furthmüller, *Comput. Mat. Sci.* **6**, 15 (1996).
- [49] L. N. Oliveira, E. K. U. Gross, and W. Kohn, *Phys. Rev. Lett.* **60**, 2430 (1988).
- [50] M. Lüders, M. A. L. Marques, N. N. Lathiotakis, A. Floris, G. Profeta, L. Fast, A. Continenza, S. Massidda, and E. K. U. Gross, *Phys. Rev. B* **72**, 024545 (2005).
- [51] M. A. L. Marques, M. Lüders, N. N. Lathiotakis, G. Profeta, A. Floris, L. Fast, A. Continenza, E. K. U. Gross, and S. Massidda, *Phys. Rev. B* **72**, 024546 (2005).
- [52] A. Floris, A. Sanna, S. Massidda, and E. K. U. Gross, *Phys. Rev. B* **75**, 054508 (2007).
- [53] R. S. Gonnelli, D. Daghero, D. Delaude, M. Tortello, G. A. Umharino, V. A. Stepanov, J. S. Kim, R. K. Kremer, A. Sanna, G. Profeta, and S. Massidda, *Phys. Rev. Lett.* **100**, 207004 (2008).
- [54] A. Sanna, G. Profeta, A. Floris, A. Marini, E. K. U. Gross, and S. Massidda, *Phys. Rev. B* **75**, 020511 (2007).
- [55] G. Profeta, C. Franchini, N. Lathiotakis, A. Floris, A. Sanna, M. A. L. Marques, M. Lüders, S. Massidda, E. K. U. Gross, and A. Continenza, *Phys. Rev. Lett.* **96**, 047003 (2006).
- [56] The phononic functional we use is an improved version with respect to Ref. [50, 51] and is discussed in Ref. [64]. In this work Coulomb interactions are included within static RPA [54], therefore excluding magnetic source of coupling[69].
- [57] The decomposition enthalpies have been computed from the predicted structures of hydrogen $P6_3m$ and $C2/c$ [11] and for sulfur and selenium on the $R3m$ and $Im3m$ reported to occur at high pressure. [2, 70–72].
- [58] J. P. Carbotte, *Rev. Mod. Phys.* **62**, 1027 (1990).
- [59] P. B. Allen and B. Mitrović (Academic Press, 1983) pp. 1 – 92.
- [60] D. A. Papaconstantopoulos, B. M. Klein, M. J. Mehl, and W. E. Pickett, ArXiv e-prints (2015), [arXiv:1501.03950](https://arxiv.org/abs/1501.03950) [cond-mat.supr-con].
- [61] Conventional implementation of the Eliashberg equations due to their computational cost, usually assume a k -independent pairing and a flat density of states. Anisotropic implementations [73] are not intrinsically affected by this limit.
- [62] P. B. Allen and R. C. Dynes, *Phys. Rev. B* **12**, 905 (1975).
- [63] W. L. McMillan, *Phys. Rev.* **167**, 331 (1968).
- [64] A. Sanna and E. K. U. Gross, (2014), to be published.
- [65] We are actually not reporting the Eliashberg result but that coming from the Allen-Dynes (AD) formula. The reason for this choice is that the two approaches agree perfectly (the difference being less than 1K) for the phonon case. But in addition when including μ^* the AD formula depends only on it, while the Eliashberg equations also depend on the Coulomb frequency cut-off (that changes the meaning of the $*$ in μ^* . If we want to use a conventional value of μ^* between 0.1 and 0.15 [59] it is then better to use the parametrized AD version of the Eliashberg method.
- [66] P. Morel and P. W. Anderson, *Phys. Rev.* **125**, 1263 (1962).

- [67] H. Suhl, B. Matthias, and L. Walker, *Physical Review Letters* **3**, 552 (1959).
- [68] P. F. McMillan, *Nat. Mat.* **1**, 1476 (2002).
- [69] F. Essenberg, A. Sanna, A. Linscheid, F. Tandetzky, G. Profeta, P. Cudazzo, and E. K. U. Gross, *Phys. Rev. B* **90**, 214504 (2014).
- [70] Y. Akahama, M. Kobayashi, and H. Kawamura, *Phys. Rev. B* **47**, 20 (1993).
- [71] Y. Akahama, M. Kobayashi, and H. Kawamura, *Phys. Rev. B* **48**, 6862 (1993).
- [72] Y. Akahama, M. Kobayashi, and H. Kawamura, *Phys. Rev. B* **56**, 5027 (1997).
- [73] E. R. Margine and F. Giustino, *Phys. Rev. B* **87**, 024505 (2013).